

## Article

# Computational Analysis of Iron Corrosion Inhibition by Compounds in Rimbang Leaf Extract (*Solanum torvum*) Using the DFT Method

### Article Info

### Article history :

Received October 17, 2024  
Revised November 12, 2024  
Accepted November 18, 2024  
Published December 30, 2024

### Keywords :

*Solanum torvum*, corrosion inhibitor, DFT, quantum parameters

Qory Sidwa Jufri<sup>1</sup>, Emriadi<sup>1\*</sup>, Imelda<sup>1</sup>

<sup>1</sup>Department of Chemistry, Faculty of Mathematics and Natural Sciences, Andalas University, Padang, Indonesia

**Abstract.** Iron is one of the most widely used metals in industry. This study was conducted on the performance of inhibitor compounds in rimbang leaf extract against iron corrosion based on several theoretical approaches. The method used is Density Functional Theory (DFT) with the basis set B3LYP/6-31G. The parameters obtained from the optimization results are  $E_{\text{HOMO}}$ ,  $E_{\text{LUMO}}$ , dipole moment, and total energy so quantum chemical parameters were obtained in the form gap energy ( $\Delta E$ ), electronegativity ( $\chi$ ), ionization potential (I), electron affinity (A), hardness ( $\eta$ ), softness ( $\sigma$ ), electrophilicity ( $\omega$ ) and nucleophilicity ( $\epsilon$ ), adsorption energy and bond energy. The calculation results showed that fisetin, alpha tocopherol-beta-d-mannoside and benzene,1-(bromomethyl)-3-nitro- were the most effective inhibitor molecules compared to other compounds. The interaction of inhibitors with Fe (110) crystals seen from the adsorption energy ( $E_{\text{ads}}$ ) and binding energy ( $E_{\text{binding}}$ ) shows that among the three best compounds contained in the rimbang extract alpha tocopherol-beta-d-mannoside has the lowest bond energy of -200.13 kJ/mol and the Inh-Fe bond length value is 1.84 Å. The bond energy and bond length values show that the interaction between the inhibitor and the Fe molecule is a chemical interaction.

This is an open access article under the [CC-BY](https://creativecommons.org/licenses/by/4.0/) license.



This is an open access article distributed under the Creative Commons 4.0 Attribution License, which permits unrestricted use, distribution, and reproduction in any medium, provided the original work is properly cited. ©2024 by author.

### Corresponding Author :

Emriadi

Department of Chemistry, Faculty of Mathematics and Natural Sciences,  
Andalas University, Padang, Indonesia

Email : [emriadi@sci.unand.ac.id](mailto:emriadi@sci.unand.ac.id)

## 1. Introduction

Corrosion affects most industrial sectors and can negatively impact the environment, safety, and security, as well as cost money each year [1]. Iron and its alloys are widely used in industrial applications and are very susceptible to corrosion [2]. The solution to this problem is to use corrosion inhibitors to reduce the corrosion rate and save yearly costs [3].

Some ways to protect iron and its alloys from corrosion include selecting suitable construction materials, coating, cathodic protection, anodic protection, and inhibitors. The development of green corrosion inhibitors is a priority for the future. This type of inhibitor does not contain heavy metals or toxic compounds. Green corrosion inhibitors can be obtained from root, seed, leaf, stem, flower, and fruit extracts which are environmentally friendly and widely available sources of organic compounds [1-4].

Corrosion inhibitors protect metals by being adsorbed on the metal surface and preventing contact with its environment thus preventing corrosion. Adsorption of inhibitors on the surface occurs through the interaction of electron pairs and phi electrons from heteroatom compounds with the iron surface. Inhibitor molecules can be adsorbed on the surface through several different mechanisms namely chemical adsorption, physical adsorption, and physicochemical adsorption so that a layer is formed that protects the metal surface from corrosion [4].

Organic compounds in plant extracts used as corrosion inhibitors contain heteroatom groups (N, O, S),  $\pi$  bonds, aromatic rings, and polar groups such as -OH, C=O [5]. For example, compounds contained in rimbang leaf extract are hexadecanoic acid, ethyl ester (11.13%), 9,12,15 octadecatrienoate acid, ethyl ester (Z,Z,Z) (7.47%) [6], DL-proline, 5-oxo-, methyl ester (9.16%), fisetin [7], alpha-tocopherol-beta-d-mannoside and other identified compounds [8] and can potentially be corrosion inhibitors.

This rimbang leaf extract has been studied by Khunbutsari *et al.* (2010) as an antibacterial [6]. Sani *et al.* (2020) tested rimbang leaf extract for treating oxidative disorders in mice [7]. Murugesan *et al.* (2021) have evaluated rimbang leaf extract for mosquito control and molecular docking potential [8]. Dharmaraj *et al.* (2021) have experimentally tested rimbang leaf extract as a corrosion inhibitor [9]. Based on the literature, no one has computationally studied the compound of rimbang leaf extract as a corrosion inhibitor.

Corrosion inhibitor testing can be done experimentally and computationally. Computation can investigate chemical problems using theoretical chemistry approaches combined with efficient computer programs to determine molecular geometry, molecular orbitals, chemical reactivity, chemical and physical properties of molecules [10]. The commonly used computational method is density functional theory (DFT) because this method is effective and its calculations are accurate [11].

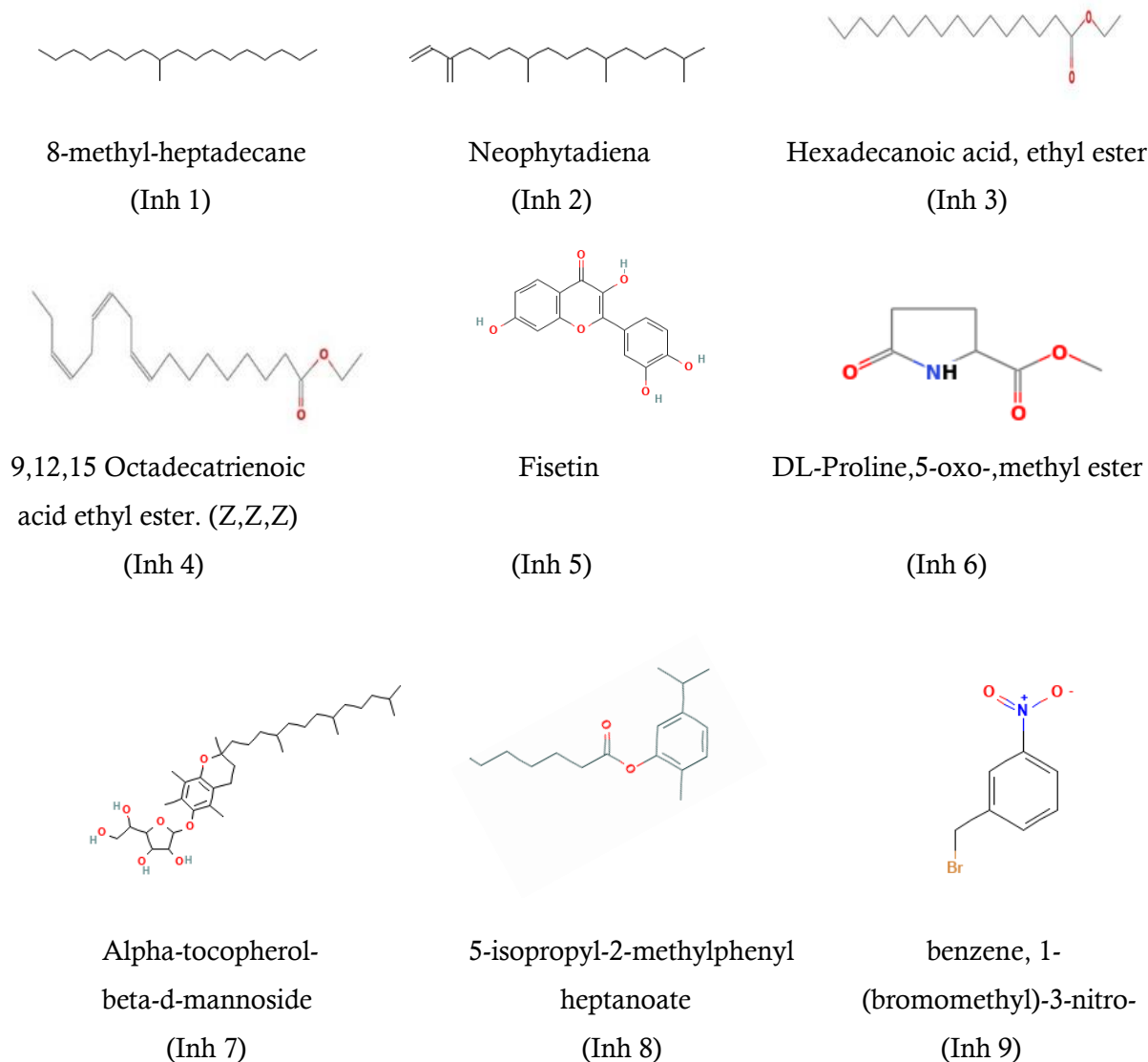
Research on iron corrosion inhibitors using computations has been conducted by Ramadhani *et al.* (2020) on xanthone derivative compounds using the DFT method [11]. Arthur (2019) researching phenyl urea derivative compounds as corrosion inhibitors using the DFT method [12], and Emriadi *et al.* (2024) researching khellin derivatives as corrosion inhibitors using the DFT method [3]. Calculations with DFT show good correlation and provide information on the quantum chemical parameters of the inhibitor compounds.

The parameters obtained from the DFT determine the corrosion inhibition ability are the highest occupied molecular orbital energy ( $E_{HOMO}$ ), the lowest unoccupied molecular orbital energy ( $E_{LUMO}$ ), and the dipole moment. From the  $E_{HOMO}$  and  $E_{LUMO}$  values obtained the gap energy ( $\Delta E$ ), electron affinity (A), electronegativity (X), hardness ( $\eta$ ), softness ( $\sigma$ ), electrophilicity ( $\omega$ ), nucleophilicity ( $\epsilon$ ) can be calculated as inhibitor reactivity parameters while the adsorption energy and bonding energy values as inhibitor parameters when interacting with Fe (110) [11]. The purpose of this study is a computational analysis of iron corrosion inhibition by compounds contained in rimbang leaf extract using the DFT method.

## 2. Experimental Section

### 2.1. Materials

The tools used in this study include hardware and software. The hardware is a Lenovo Ideapad Slim 1i laptop with specifications Intel(R) Celeron(R) N4020 CPU @ 1.10GHz RAM 8.00 GB, and the software is a Gaussian 16W program to process data and Gaus View 6.0 to optimize the content of rimbang leaf extract compounds and the Vesta program to make Fe (110) crystals. The materials used in the study were rimbang leaf extract compounds from the journal [6–8], as shown in figure 1.



**Figure 1.** Structure of compounds contained in rimbang leaf extract

### 2.2. Geometry Optimization of Rimbang Leaf Extract Compounds

The compounds in the extract of rimbang leaves were optimized using the Gaussian 16W program package, DFT calculation method, and B3LYP/6-31G basis set in solvent free conditions. After the optimization, the data will be stored in 3 formats: chk, gif, and notepad. The output data is in the form of optimal geometric structure,  $E_{\text{HOMO}}$ ,  $E_{\text{LUMO}}$ , countour HOMO (Highest Occupied Molecular

Orbital) and LUMO (Lowest Unoccupied Molecular Orbital), total energy ( $E_{tot}$ ), dipole moment ( $\mu$ ), and ESP (Electrostatic Potential). Then, from the  $E_{HOMO}$   $E_{LUMO}$  values, the inhibitor reactivity parameters are obtained in the form of band gap values ( $\Delta E$ ), electronegativity ( $\chi$ ), hardness ( $\eta$ ), softness ( $\sigma$ ), electrophilicity ( $\omega$ ), nucleophilicity ( $\epsilon$ ). After calculation, the compound with the best inhibitory ability is obtained, and the stability of the inhibitor is analyzed.

### 2.3. Optimization of Compounds from Rimbang Leaf Extract Interacting with Fe (110) Crystals

The Fe (110) crystal structure is made using Vesta software, and then the file is saved in pdb format. The Fe (110) crystal is then opened in the Gauss view 6.0 window and interacted with the inhibitor molecule. The Fe-Inhibitor complex is then optimized using the molecular mechanics method. The optimization results are in the form of optimal geometric structures and total energy. Then, from the total energy value, the interaction energy and bonding energy values of the compound are obtained to analyze the interaction and bonding of the inhibitor with the Fe (110) crystals.

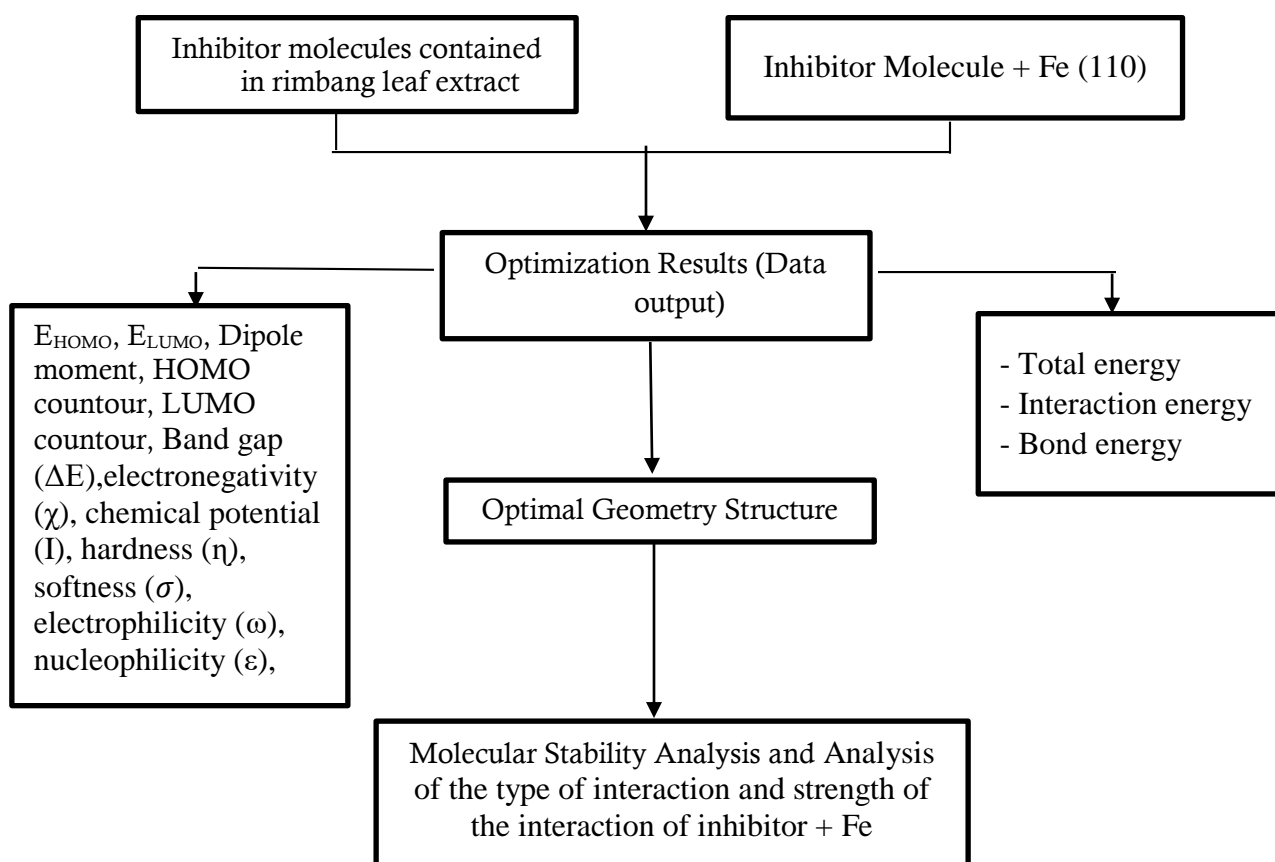


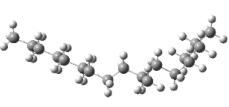
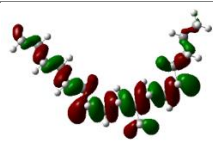
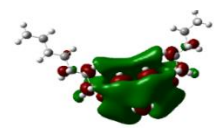

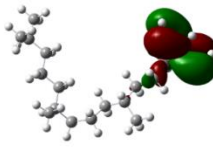
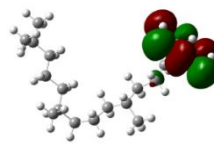
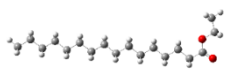
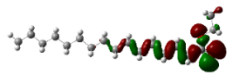
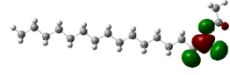
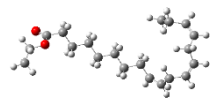
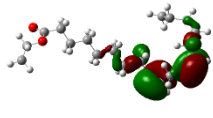
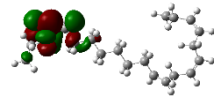
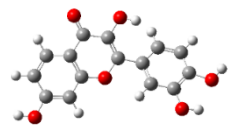
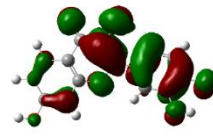
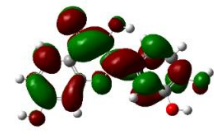
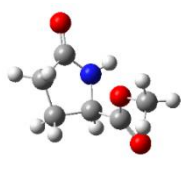
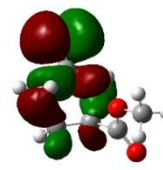
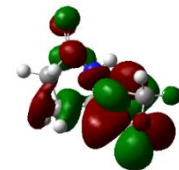
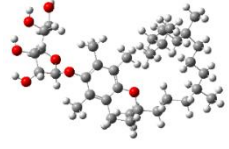
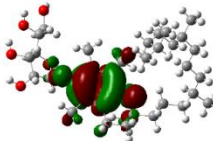
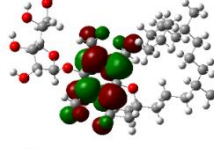
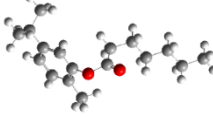
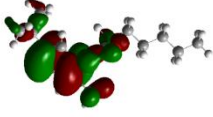
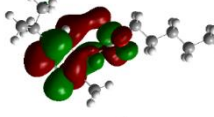
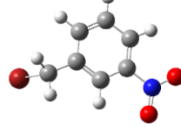
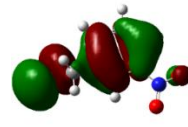
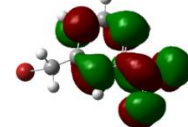
Figure 2. Research flow diagram

## 3. Results and Discussion

### 3.1 Geometry Optimization and Contour HOMO-LUMO

This optimization was done using the DFT method to obtain a stable molecular structure. The optimal geometric structure, HOMO and LUMO contours of compounds in rimbang leaves in the solvent free phase in the 3D form are shown in table 1. The geometric structure with red atom color = O; gray = C; white = H; blue = N; dark red = Br, while the HOMO-LUMO Contour in the compound is green = bonding orbital and red = antibonding orbital.

**Table 1.** Geometric structure, HOMO, and LUMO contour of compounds contained in rimbang leaves. Compound Geometry Structure

Inh	Compound	Geometry Structure	Contour HOMO	Contour LUMO
1	8 methyl heptadecane			
2	Neophytadiena			
3	Hexadecenoic acid, ethyl ester			
4	9,12,15 octadecatrienoic acid etyl ester			
5	Fisetin			
6	DL-Prolin, 5-oxo-, metil ester			
7	Alpha tocopherol-beta-d-mannoside			
8	5-isopropil 2 metilfenil heptanoate			
9	Benzene, 1-(bromometil)-3-nitro-			

The compounds in rimbang leaf extract are a group of metabolite compounds, namely flavonoids, fatty acids, phenolics, diterpenes, and vitamins, which in their structure contain hydroxyl groups (-OH), carboxyl groups (-COOH) and carbonyl groups (-C=O). Compounds containing functional

groups such as carbonyl and aromatic rings and conjugated  $\pi$  electrons act as corrosion inhibitors due to forming coordination bonds with empty d orbitals on the metal surface [13].

The HOMO contour is the electron density in the HOMO band and shows the area that is an electron donor. In contrast, the LUMO contour is the electron density in the LUMO band and shows the area that is an electron acceptor [14].

The HOMO and LUMO contours of the nine inhibitor molecules are distributed almost the same namely on the -C-C- group for Inh 1, on the -C=C- group for Inh 2, on the carboxyl group for Inh 3 and 4, on the aromatic ring for Inh 7 and 8, while the other Inh are distributed throughout the molecular structure. This indicates that all of these compounds have active groups distributed on the molecule and can increase the absorption of inhibitors. Similar observations have been reported in the literature [15] the compound 6-methyl-2-(p-tolyl)-1,4-dihydroquinoxaline has HOMO and LUMO contours distributed throughout the structure.

### 3.2 Parameters of Inhibitor Reactivity of Rimbang Leaf Extract Compounds

The reactivity of a corrosion inhibitor can be computationally determined from the values of  $E_{\text{HOMO}}$ ,  $E_{\text{LUMO}}$ , bandgap ( $\Delta E$ ), electronegativity ( $\chi$ ), ionization potential (I), electron affinity (A), hardness ( $\eta$ ), softness ( $\sigma$ ), electrophilicity ( $\omega$ ) and nucleophilicity ( $\epsilon$ ) as shown in table 2.

**Tabel 2.** Calculation values of inhibitor reactivity parameters

Parameters	Compound content of rimbang leaf extract								
	Inh 1	Inh 2	Inh 3	Inh 4	<b>Inh 5</b>	Inh 6	<b>Inh 7</b>	Inh 8	<b>Inh 9</b>
$E_{\text{HOMO}}$ (eV)	-7.82	-6.11	-7.24	-6.45	-5.85	-6.71	<b>-5.42</b>	-6.54	-7.58
$E_{\text{LUMO}}$ (eV)	2.35	-0.56	-0.02	-0.03	-1.78	-0.68	0.23	-0.33	<b>-3.09</b>
$\Delta E$ (eV)	10.18	5.54	7.21	6.42	<b>4.07</b>	6.02	5.66	6.21	4.48
$\chi$ (eV)	2.73	3.34	3.63	3.24	3.82	3.69	<b>2.59</b>	3.44	5.34
I (eV)	7.82	6.11	7.24	6.45	5.85	6.71	<b>5.42</b>	6.54	7.58
A (eV)	-2.35	0.56	0.02	0.03	1.78	0.68	-0.23	0.33	<b>3.09</b>
$\eta$ (eV)	5.09	2.77	3.60	3.21	<b>2.03</b>	3.01	2.83	3.10	2.24
$\sigma$ (eV <sup>-1</sup> )	0.19	0.36	0.27	0.31	<b>0.49</b>	0.33	0.35	0.32	0.44
[16] $\omega$ (eV)	-0.68	-0.83	-0.90	-0.81	-0.95	-0.92	<b>-0.64</b>	-0.86	-1.33
$\epsilon$ (eV <sup>-1</sup> )	-1.46	-1.19	-1.10	-1.23	-1.04	-1.08	-1.54	-1.16	<b>-0.74</b>

The HOMO orbital energy is the ability of a molecule to donate electrons to an acceptor with an empty molecular orbital. Conversely, the LUMO orbital energy is related to electron affinity with the tendency to accept electrons [17]. The greater the HOMO energy value, the more inhibitor electrons are donated. The smaller the LUMO energy value, the greater the number of electrons the inhibitor receives. Higher HOMO energy values have better corrosion inhibition performance [18].

The calculated  $E_{\text{HOMO}}$  and  $E_{\text{LUMO}}$  values for the compounds are shown in table 2. From these results the best compounds according to  $E_{\text{HOMO}}$  are inh 7 and inh 5 with values of -5.42 eV and -5.85 eV respectively. Inh 7 and inh 5 can be associated with the presence of many OH groups that are effective as electron donors. This indicates that inh has a high tendency to donate electrons to the low and unfilled d orbitals of metal atoms [16]. In addition, inh 9 shows a stable  $E_{\text{LUMO}}$  for forming back bonds with metals.

Bandgap ( $\Delta E$ ) is the ratio between  $E_{\text{HOMO}}$  and  $E_{\text{LUMO}}$  indicating stability as a corrosion inhibitor. A smaller bandgap value of the inhibitor molecule will improve inhibition efficiency because of the energy required to excite electrons from the lowest to the highest orbital. Inh 5 and 9 show the lowest

bandgap (4.07 and 4.48 eV respectively) indicating their high reactivity and kinetic stability [16],[19]. The band gap can be calculated using equation (1).

Electronegativity ( $\chi$ ) is an important descriptor when a reaction occurs between a metal and an inhibitor molecule. Electronegativity indicates the capacity of a molecule to attract electrons in a covalent bond. The smaller the electronegativity value the more difficult it is to attract electrons from the metal and its stability is high [12]. Inh 7 shows a lower electronegativity value of 2.59 eV than iron (electronegativity 7 eV). The further the inhibitor electronegativity value is from the metal, the better its reactivity and the greater the corrosion inhibition efficiency [16]. The electronegativity value is obtained from equation (2).

$$\Delta E = E_{\text{LUMO}} - E_{\text{HOMO}} \quad (1)$$

$$\chi = \frac{I + A}{2} \quad (2)$$

$$I = -E_{\text{HOMO}} \quad (3)$$

$$A = -E_{\text{LUMO}} \quad (4)$$

$$\eta = \frac{I - A}{2} \quad (5)$$

$$\sigma = \frac{1}{\eta} \quad (6)$$

$$\omega = \frac{\mu^2}{2\eta} \quad (7)$$

$$\varepsilon = \frac{1}{\omega} \quad (8)$$

Ionization potential (I) is the energy required to remove an electron from the highest occupied molecular orbital (HOMO). Higher ionization potential values indicate less reactive molecules and lower values can more easily donate electrons to the metal surface [20]. From table 2. Corrosion inhibitors show good ionization potentials, namely inh 5 and 7 (5.85 and 5.42 eV respectively). It can be observed that the hydroxyl groups in inh 5 and 7 significantly decrease the ionization potential values. The ionization potential values are obtained from equation (3).

Electron affinity (A) is the energy released when an electron is added to the lowest unoccupied molecular orbital (LUMO). A high value of electron affinity indicates the ability of the inhibitor to accept electrons from the metal surface so that they are stable during the interaction of the inhibitor with the metal and can participate efficiently in the electron donor and acceptor process [20]. Inh 9 shows the highest value (3.09 eV) because there is a nitro group as a strong electron withdrawer so that it is good in the process of donating and accepting electrons from the metal. The Electron affinity value is obtained from equation (4).

Hardness ( $\eta$ ) indicates its resistance to deformation or distortion of the electron cloud. Molecules with lower hardness are generally more reactive and more suitable for corrosion inhibitors because they can easily donate electrons or accept electrons and are inversely proportional to softness. High softness values indicate efficiency as suitable inhibitors against metal surfaces [21-22]. Inh 5 and 9 show the lowest hardness (2.03 and 2.24 eV) and the highest softness (0.49 and 0.44 eV<sup>-1</sup> respectively). The hardness and softness value is obtained from equation (5) and (6).

Electrophilicity ( $\omega$ ) measures the tendency to accept additional electrons and the resistance of a system to exchange electrons with its environment. A high electrophilicity value indicates a high electron transfer between the donor and acceptor [23-24]. Inh 7 has the highest value (-0.64 eV) indicating a high ability to accept electrons. The electrophilicity value is obtained from equation (7).

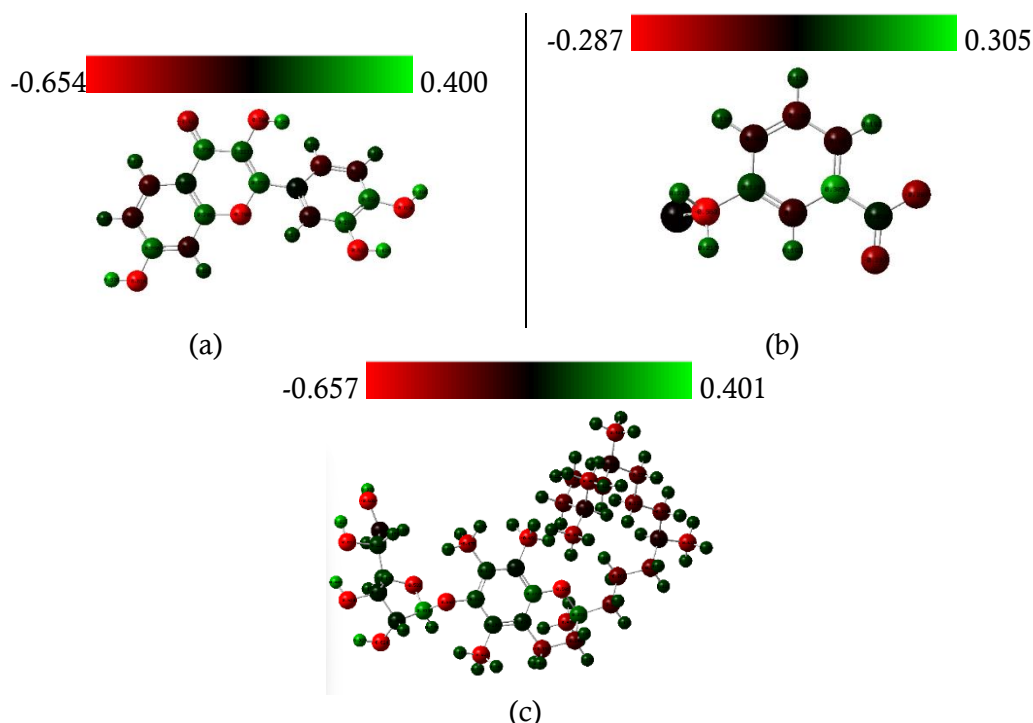
Nucleophilicity ( $\varepsilon$ ) indicates the tendency to donate electrons with others or the opposite of electrophilicity. High nucleophilicity values make good candidates as corrosion inhibitors [25-26]. The

highest nucleophilicity value is inh 9 indicating that the molecule can easily donate electrons to the metal. The nucleophilicity value is obtained from equation (8).

In conclusion, the nine most reactive compounds of rimbang leaf extract are inh 5, inh 7 and inh 9 (fisetin, alpha tocopherol-beta-d-mannoside and benzene 1-(bromomethyl)-3-nitro-). Inh 5 has many hydroxyl groups that will donate electrons and aromatic rings whose electrons are conjugated so that they help the process of donating electrons to metals just like inh 7 because molecules containing heteroatoms and heterocycles are more effective as corrosion inhibitors than only containing aliphatic chains such as the molecular structure of inh 1. Inh 9 contains a nitro group as an electron withdrawer, an aromatic ring as a weak electron donor and a Br atom that attracts electrons from adjacent groups. Therefore, the three compounds will be tested for Mulliken charge density and their interactions with Fe (110) crystals.

### 3.3 Mulliken Charge Density

Figure 3 shows the mulliken density value of the compounds contained in the extract of rimbang leaves. The atom with the highest negative charge illustrates that the inhibitor readily donates electrons to the metal surface. However, it can be seen that the inhibitor can easily interact with the metal surface through the active center (O atom). The values obtained indicate that the O atom has a higher negative charge on inh 5 (fisetin), inh 7 (alpha tocopherol-beta-d-mannoside) and inh 9 (benzene 1-(bromomethyl)-3-nitro-) which indicates that the compounds of rimbang leaves extract effectively inhibit corrosion by being adsorbed on the metal surface through their active groups [27-28].



**Figure 3.** Mulliken density of rimbang leaf extract (a) Fisetin (b) Benzene, 1-(bromomethyl)-3-nitro (c) Alpha tocopherol-beta-d-mannoside

The fisetin compound has the most negative O atomic charge, which is -0.654 on the O28 atom, the benzene 1-(bromomethyl)-3-nitro- compound, has the most negative O atomic charge on the O17 atom with a value of -0.287 and the alpha tocopherol-beta-d-mannoside compound has the most negative O atomic charge on the O96 atom with a value of -0.657. Of the three compounds, the most

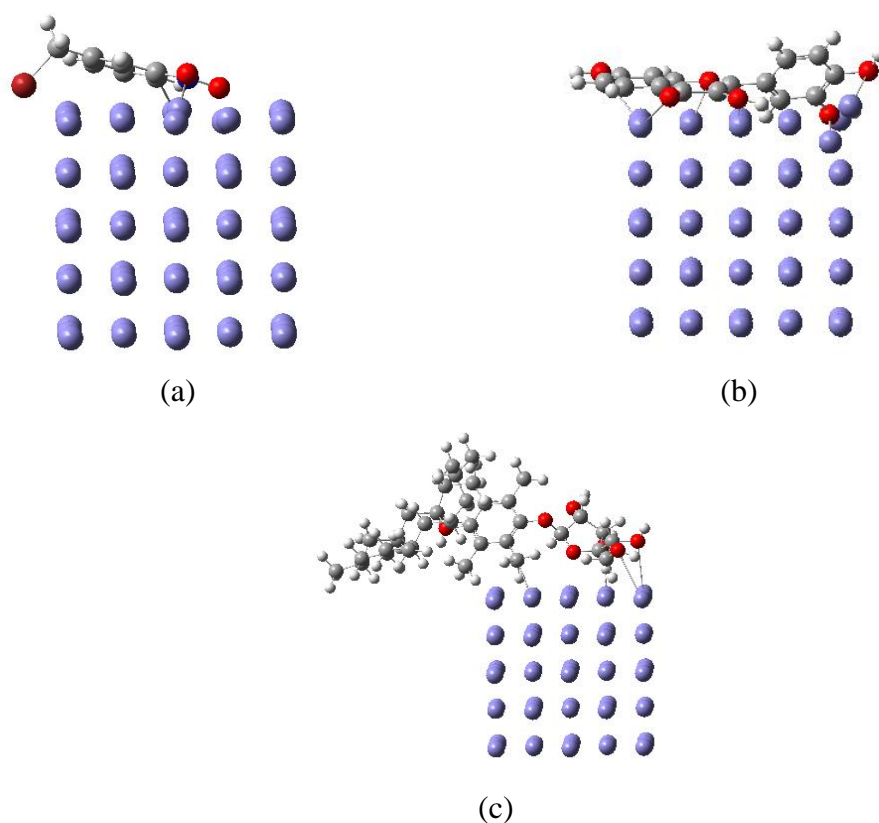


negative atomic charge value is found in the Alpha tocopherol-beta-d-mannoside compound, which shows the compound's better ability to donate electrons to the metal surface.

### 3.4 Interaction of Inhibitors with Fe (110)

This study used Fe (110) crystals to analyze the interaction of rimbang leaf extract content inhibitors as corrosion inhibitors on iron. Optimization was carried out on each molecule, Fe crystals, and combinations of molecules with Fe crystals to determine the interaction between molecules and inhibitors.

Figure 4 shows the inhibitor molecules adsorbed on the iron surface in a flat orientation. The central site of inhibitor adsorption on the Fe (110) surface through the oxygen heteroatom group and aromatic ring structure interact parallel or flat with the iron surface.



**Figure 4.** Interaction of inhibitors with Fe (110) (a) benzene, 1-(bromomethyl)-3-nitro (b) fisetin (c) alpha tocopherol-beta-d-mannoside.

Optimization was carried out using the molecular mechanics method to obtain the Fe energy value, the inhibitor molecule energy value, and the Fe-inhibitor complex energy value. The adsorption value and bond value were determined based on the formulas in equations (9) and (10) and the bond length between Fe and O, as shown in table 3.

The performance of inhibitor adsorption on the iron surface is analyzed based on adsorption energy and bond energy. The negative value of bond energy indicates that the inhibitor molecules on the Fe (110) surface are spontaneously adsorbed. The more positive the adsorption energy, the more negative the bond energy indicates that it is easier for the molecules to be adsorbed on the iron surface [3].

$$\text{Adsorption energy} = E_{\text{complex}} - (E_{\text{Fe}} + E_{\text{inhibitor}}) \quad (9)$$

$$\text{Bonding energy} = -E_{\text{adsorption}} \quad (10)$$

The higher adsorption energy value and lower binding energy value are found in the alpha tocopherol-beta-d-mannoside compound because it has many OH groups and has an aromatic ring and long carbon chain, making it easier for oxygen atoms to donate electrons to Fe molecules.

**Tabel 3.** The interaction value of inhibitor molecules with Fe (110)

Inhibitor	$E_{\text{ads}}$ (kJ/mol)	$E_{\text{binding}}$ (kJ/mol)	r Fe-O (Å)
Fisetin	183.50	-183.50	1.86
Alpha tocopherol-beta-d-mannoside	<b>200.13</b>	<b>-200.13</b>	<b>1.84</b>
Benzene, 1-(bromometil)-3-nitro-	155.18	-155.18	1.86

The negative sign indicates that the bond formation process occurs exothermically. Based on the bond energy value, it is known that the three inhibitor compounds with Fe crystals are chemical interactions. One of the factors that determines the type of physisorption or chemisorption that can occur is the closest distance between the inhibitor atom and the Fe atom. The estimate for the type of physisorption is determined when the inhibitor-surface distance is  $>3\text{\AA}$ , while the type of chemisorption is determined when the distance is  $<3\text{\AA}$  [29-30]. From the results obtained, the bond length of the inhibitor compound shows almost the same value, and the interaction that occurs is a chemical interaction.

#### 4. Conclusion

Alpha tocopherol-beta-d-mannoside, fisetin, and benzene, 1-(bromomethyl)-3-nitro compounds are effective inhibitor molecules among other inhibitor molecules in rimbang leaf extract compounds based on the reactivity parameters of the inhibitor compounds. Meanwhile, the interaction of the inhibitor with Fe (110) shows that among the three compounds, the one with the lowest bond energy value of -200.13 kJ/mol and the smallest Inh-Fe bond length value of 1.84 Å is alpha tocopherol-beta-d-mannoside. The bond energy and bond length values show that the interaction between the inhibitor and the Fe molecule is a chemical interaction.

#### References

- [1] Bouoidina, A., Ech-chihbi, E., El-Hajjaji, F., El Ibrahim, B., Kaya, S., and Taleb, M. (2021). Anisole derivatives as sustainable-green inhibitors for mild steel corrosion in 1 M HCl: DFT and molecular dynamic simulations approach. *Journal of Molecular Liquids*. 324.
- [2] Berrissoul, A., Loukili, E., Mechbal, N., Benhiba, F., Guenbour, A., Dikici, B. (2020). Anticorrosion effect of a green sustainable inhibitor on mild steel in hydrochloric acid. *Journal of Colloid and Interface Science*. 580 740–752.
- [3] Marni, L.G., Emriadi, E., Imelda, I., Darajat, S., and Khoiriah, K. (2024). Theoretical Study of Khellin Derivatives as Corrosion Inhibitors Based on Density Functional Theory (DFT). *Turkish Computational and Theoretical Chemistry*. 8 (4), 36–47.
- [4] Golafshani, M.G., Tavakoli, H., Hosseini, S.A., and Akbari, M. (2023). MD and DFT computational simulations of Caffeoylquinic derivatives as a bio-corrosion inhibitor from quince extract with experimental investigation of corrosion protection on mild steel in 1M H<sub>2</sub>SO<sub>4</sub>. *Journal of Molecular Structure*. 1275.

- 
- [5] Berrissoul, A., Ouarhach, A., Benhiba, F., Romane, A., Guenbour, A., Outada, H., et al. (2022). Exploitation of a new green inhibitor against mild steel corrosion in HCl: Experimental, DFT and MD simulation approach. *Journal of Molecular Liquids*. 349.
- [6] Khunbutsri, D., Naimon, N., Satchasataporn, K., Inthong, N., Kaewmongkol, S., Sutjarit, S. (2022). Antibacterial Activity of Solanum torvum Leaf Extract and Its Synergistic Effect with Oxacillin against Methicillin-Resistant Staphylococci Isolated from Dogs. *Antibiotics*. 11 (3).
- [7] Sani, S., Lawal, B., Ejeje, J.N., Aliu, T.B., Onikanni, A.S., Uchewa, O. (2022). Biochemical and tissue physiopathological evaluation of the preclinical efficacy of Solanum torvum Swartz leaves for treating oxidative impairment in rats administered a  $\beta$ -cell-toxicant (STZ). *Biomedicine and Pharmacotherapy*. 154.
- [8] Murugesan, R., Vasuki, K., and Kaleeswaran, B. (2023). A green alternative: Evaluation of Solanum torvum (Sw.) leaf extract for control of Aedes aegypti (L.) and its molecular docking potential. *Intelligent Pharmacy*.
- [9] Dharmaraj, R., Raga Samuyktha, S.A., Thansiya, K., Syed Manzoor, S., Naveen Kumar, B., and Maruvarasan, S. (2021). Turkey Berries Leaves Extract as Corrosion Inhibitor Embedded Steel in Concrete. *IOP Conference Series: Materials Science and Engineering*. 1145 (1), 012073.
- [10] Ayalew, M.E. (2022) DFT Studies on Molecular Structure, Thermodynamics Parameters, HOMO-LUMO and Spectral Analysis of Pharmaceuticals Compound Quinoline (Benzo[b]Pyridine). *Journal of Biophysical Chemistry*. 13 (03), 29–42.
- [11] Ramadhani, F., Emriadi, and Syukri. (2020). Theoretical Study of Xanthone Derivative Corrosion Inhibitors Using Density Functional Theory (DFT). *Jurnal Kimia Valensi*. 6 (1), 95–103.
- [12] Arthur, D.E., Uzairu, A., Mustapha, A., Adeniji, E.S., and David, E.A. (2019). A Computational adsorption and DFT studies on corrosion inhibition potential of some derivatives of phenyl-urea 5, 19-32.
- [13] Feng, L., Yao, H., Ma, X., Zhu, H., and Hu, Z. (2023). Effect of three penicillin-based as corrosion inhibitors on Q235 steel in hydrochloric acid. *International Journal of Electrochemical Science*. 18 (12).
- [14] Radhi, A.H., Du, E.A.B., Khazaaal, F.A., Abbas, Z.M., Aljelawi, O.H., Hamadan, S.D., et al. (2020). HOMO-LUMO energies and geometrical structures effecton corrosion inhibition for organic compounds predict by DFT and PM3 methods. *NeuroQuantology*. 18 (1), 37–45.
- [15] Benhiba, F., Hsissou, R., Benzikri, Z., Echihi, S., El-Blilak, J., Boukhris, S. (2021). DFT/electronic scale, MD simulation and evaluation of 6-methyl-2-(p-tolyl)-1,4-dihydroquinoxaline as a potential corrosion inhibition. *Journal of Molecular Liquids*. 335 116539.
- [16] Oyenyin, O.E., Ojo, N.D., Ipinloju, N., Agbaffa, E.B., and Emmanuel, A.V. (2022). Investigation of the corrosion inhibition potentials of some 2-(4-(substituted)arylidene)-1H-indene-1,3-dione derivatives: density functional theory and molecular dynamics simulation. *Beni-Suef University Journal of Basic and Applied Sciences*. 11 (1).
- [17] Abdul Hussein, E., Fanfoon, D.Y., Al-Uqaily, R.A.H., Salman, A.M., Kadhim, M.M., Salman, A.W. (2021). 1-Isoquinolinyl phenyl ketone as a corrosion inhibitor: A theoretical study. in: *Mater Today Proc, Elsevier Ltd*. 2241–2246.
- [18] Chen, X., Chen, Y., Cui, J., Li, Y., Liang, Y., and Cao, G. (2021). Molecular dynamics simulation and DFT calculation of “green” scale and corrosion inhibitor. *Computational Materials Science*. 188.
- [19] Ouakki, M., Galai, M., Rbaa, M., Abousalem, A.S., Lakhrissi, B., Rifi, E.H. (2019). Quantum chemical and experimental evaluation of the inhibitory action of two imidazole derivatives on mild steel corrosion in sulphuric acid medium. *Heliyon*. 5 (11).
-

- [20] Aljibori, H.S., Alamiery, A., Gaaz, T.S., and Al-Azzawi, W.K. (2024). Exploring corrosion protection for mild steel in HCl solution: An experimental and theoretical analysis of an antipyrine derivative as an anticorrosion agent. *Carbon Neutralization*. 3 (1), 74–93.
- [21] Al-Amiery, A., Betti, N.A., and Shaker, L.M. (2024). Exploring the effectiveness of 3-chloro-4-morpholin-4-yl-1,2,5-thiadiazole as an eco-friendly corrosion inhibitor for mild steel in HCl solution: Experimental and DFT analysis. *Results in Engineering*. 24 (9).
- [22] Ibrahim, M.A.A., Moussa, N.A.M., Mahmoud, A.H.M., Sayed, S.R.M., Sidhom, P.A., Abd El-Rahman, M.K. (2023). Density functional theory study of the corrosion inhibition performance of 6-mercaptopurine and 6-thioguanine expired drugs toward the aluminium (111) surface. *RSC Advances*. 13 (41), 29023–29034.
- [23] Hadigheh Rezvan, V. (2024). Molecular structure, HOMO–LUMO, and NLO studies of some quinoxaline 1,4-dioxide derivatives: Computational (HF and DFT) analysis. *Results in Chemistry*. 7 (12), 101437.
- [24] Ahamed, J. I., Ramkumaar, G. R., Kamalarajan, P., Narendran, K., Valan, M. F., Sundareswaran, T., ... & Bharathi, S. (2022). Novel quinoxaline derivatives of 2, 3-diphenylquinoxaline-6-carbaldehyde and 4, 4'-(6-methylquinoxaline-2, 3-diyl) bis (N, N-diphenylaniline): Synthesis, structural, DFT-computational, molecular docking, antibacterial, antioxidant, and anticancer studies. *Journal of Molecular Structure*, 1248, 131418.
- [25] Guo, L., Safi, Z.S., Kaya, S., Shi, W., Tüzün, B., Altunay, N. (2018). Anticorrosive effects of some thiophene derivatives against the corrosion of iron: A computational study. *Frontiers in Chemistry*. 6 (5).
- [26] Shah, R., & Verma, P. K. (2019). Synthesis of thiophene derivatives and their anti-microbial, antioxidant, anticorrosion and anticancer activity. *BMC chemistry*, 13, 1-13.
- [27] Abdallah, M., Al Bahir, A., Altass, H.M., Fawzy, A., El Guesmi, N., Al-Gorair, A.S. (2021). Anticorrosion and adsorption performance of expired antibacterial drugs on Sabic iron corrosion in HCl solution: Chemical, electrochemical and theoretical approach. *Journal of Molecular Liquids*. 330 115702.
- [28] Feng, L., Zhang, S., Tao, B., Tan, B., Xiang, B., Tian, W., & Chen, S. (2020). Two novel drugs as bio-functional inhibitors for copper performing excellent anticorrosion and antibacterial properties. *Colloids and Surfaces B: Biointerfaces*, 190, 110898.
- [29] Al-Qurashi, O.S. and Wazzan, N. (2022). Molecular and periodic DFT calculations of the corrosion protection of Fe(1 1 0) by individual components of Aerva lanata flower as a green corrosion inhibitor. *Journal of Saudi Chemical Society*. 26 (6).
- [30] Mazurek, A. H., Szeleszczuk, Ł., & Pisklak, D. M. (2020). Periodic DFT calculations—review of applications in the pharmaceutical sciences. *Pharmaceutics*, 12(5), 415.